POLISH MARITIME RESEARCH 2 (102) 2019 Vol. 26; pp. 6-14
10.2478/pomr-2019-0020

CENTRIFUGAL COMPRESSOR PERFORMANCE IMPROVEMENT THROUGH MULTI SPLITTER IMPELLER

Adil Malik[1]
Qun Zheng[1]
Shafiq R. Qureshi[2]
Salman A. Ahmed[1]
D. KB Gambo[1]
[1] Harbin Engineering University, Harbin, China
[2] National University of Sciences and Technology, Karachi, Pakistan

ABSTRACT

In the paper, a back swept impeller of centrifugal compressor is experimentally studied and numerically validated and modified to increase its pressure ratio and improve efficiency, as well as to analyse the effect of splitter blade location between two main blades. The back swept multi splitter blade impeller was designed with a big splitter positioned close to the main blade suction surface and a smaller splitter close to the pressure surface. Adding this multi splitter improves the overall performance of the modified impeller due to less intensive flow separation and smaller pressure loss. In particular, the total pressure ratio was observed to increase from 4.1 to 4.4, with one percent increase in efficiency.

Keywords: Centrifugal compressor; back swept impeller; flow separation; efficiency; numerical simulation

INTRODUCTION

In recent years, a lot of 3D numerical simulation studies have been done to increase the pressure ratio in compressors. These studied aimed at identifying unknown losses in radial compressor aerothermodynamics and estimating various fluid flow characteristics [1, 2, 3, 4, 5, 11, 17]. Definite estimations of the internal fluid flow field which were made by Dean [8], Hathaway et al. [10], Kano et al. [12], Krain [13], Moore et al. [18], Skoch et al. [20], and Vavra [23] were extremely helpful in filling holes of unknown phenomena in fluid flows in compressors. The centrifugal compressor design is restricted by the inlet Mach number limitation and flow separation near the trailing edge close to the shroud. Arrangements of shorter blades, called "1/2 blades" or "splitter blades", are designed in passages between the two full-length blades to reduce flow separation in the impeller. In the passages between the full blades, a set of splitter blades is introduced symmetrically in the mid of the channel. There are very limited studies to address the effect of splitter location on compressor performance.

Centrifugal compressors used in marine machinery differ from industrial applications. They are utilized in almost all turbo chargers of diesel engines onboard ships. Centrifugal compressor designers use splitters to achieve higher pressure ratio and avoid flow choking in the throat at the main blade leading edge in radial impellers [6, 7]. The conventional design approach for the splitter is to use the same blade profile for the full and splitter blades, with the splitter placed at mid-pitch of the two main blades. Studies on the introduction of splitter vanes in the impeller passage have been conducted in the past [9, 14, 15, 17, 22]. Fradin [9] investigated broadly the transonic stream in two centrifugal rotors: with and without splitters. The arrangement of a splitter was similar to that of the main blades, and its location was at the centre between two main blades. The studies have revealed that the flow field at impeller outlet is more consistent after applying splitters. The splitter compressor has better performance than that without splitter. Millour [17] examined the same configuration by using a three-dimensional flow analysis. He demonstrated that the main effects of using splitters include the decrease of the impeller blade load and smaller jet/wake impact at the impeller trailing edges.

Tamaki et al. [21] utilized splitter blades with different camber angle at inducer than that of the main blade in the radial impeller design with pressure ratio of 4.3. He achieved enhanced blade loading distribution and efficiency. By changing blade thickness and shape, Ona et al. [19] retrofitted the compressor and succeeded in reducing rapid fluid flow acceleration/deceleration at leading edge and separation phenomena at hub.

The splitter compressor has better performance than that without splitter. A number of researchers have studied the effect of splitters arranged in pairs, but splitters with different sizes have not been examined so far. To fill this gap, an arrangement of big and small splitter is studied in the article. The structure of the back swept impeller used in the experiment was modified by adding a big splitter close to the main blade suction surface and a smaller splitter close to the pressure surface. The splitters were designed using the same blade profiles as the main blades. The multi splitter was applied in a centrifugal impeller with vaneless diffuser to investigate the effect of splitter location between two main blades on centrifugal compressor performance in terms of pressure ratio increase and efficiency improvement. All flow conditions were kept the same as in the experimentally validated impeller.

VALIDATION OF NUMERICAL SIMULATION

The high pressure ratio back swept impeller which had been experimentally studied by Mckain and Holbrook, and analysed numerically with the CFD code ADPAC by L. M Larosiliere, Skoch and Prahst was selected to validate the CFD code and simulation procedure. The impeller parameters are listed in Table 1:

Tab. 1. Impeller parameters

No.	Parameter	Value
1.	Pressure ratio	4
2.	Mass flow	4.54 kg/sec
3.	RPM	21789
4.	Specific speed	0.60
5.	Impeller tip speed	492 m/sec
6.	No. of main blades	15
7.	No. of splitter blades	15
8.	Impeller exit diameter	0.431 m
9.	Tip clearance at trailing edge	0.000203 m
10.	Tip clearance at leading edge	0.0001524 m
11.	Backswept from radial	50 degrees

The pictorial view of the original impeller is given in Fig. 1, with monitoring points indicated. The blade coordinates, as well as the details of aerodynamic design and mechanical specifications are taken from McKain and Holbrook [16].

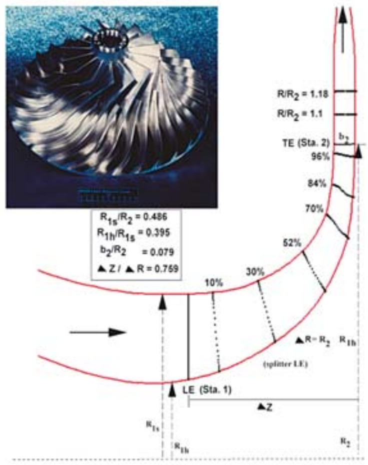

Fig. 1. Original impeller sketch with monitoring points

COMPUTATIONAL METHOD

The computational simulation of the experimental impeller was performed using Ansys CFX 18. The blade geometry as reported by McKain and Holbrook [16] was used to construct the model in Ansys Blade Gen 18. Fig. 2 shows the 3-D model and the meridional view, while Fig. 3 shows the blade-to-blade view of the impeller in Ansys Blade Gen. The computational model reveals some variation from the original impeller in which the blade profile and thickness differ slightly between the splitter blade and the main blade. Due to certain software restrictions, the computational model of splitters was created using the same profile and thickness definition as per the main blade.

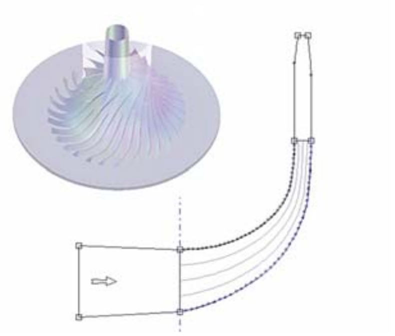

Fig. 2. 3-D model and meridional view of impeller

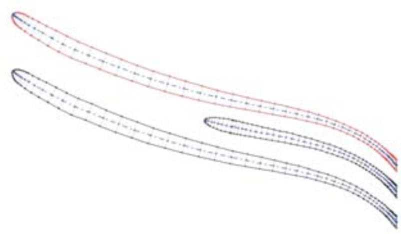

Fig. 3. Blade-to-blade view of impeller

The model was exported to Ansys Turbo Grid for meshing. In the generated fine mesh, the total number of nodes was 1084655, the total number of elements was 1027008, and the number of hexahedrons was 1027008. Figs. 4 and 5 show the inlet mesh and the mesh at shroud including tip clearance. The size of the computational clearance is a bit different from that measured. In the experiment, the shroud clearance was 0.1524 mm at impeller inlet, 0.61 mm at mid-stream, and 0.203 mm at outlet. In the computational grid, it is also set at 0.1524 mm at impeller blade leading edge and 0.203 mm at impeller outlet. However, the mid span clearance may differ from the measured value. Keeping in mind the final goal, which was restricting the reversal flow at outlet, the outlet boundary of the vaneless diffuser is slightly contracted.

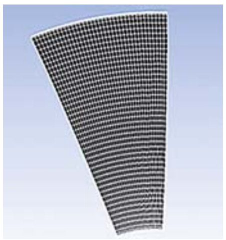

Fig. 4. Inlet mesh

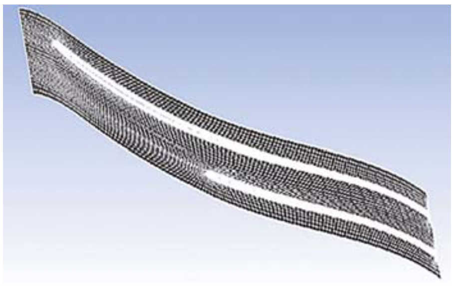

Fig. 5. Mesh at shroud including tip clearance

The mesh model was exported to Ansys CFX Pre. The total pressure and temperature at the inlet boundary were specified based on the experiment. The flow direction was set at zero swirl angle. The mass flow of 4.54 kg/sec was assumed at the exit of the computational domain. The solution results were obtained by solving the 3D steady compressible Reynolds-Averaged Navier–Stokes (RANS) equations, complemented with the SST turbulence model with gamma theta transitional turbulence. A finite-volume method was used to discretize the equations. Air was treated as ideal gas. A high-resolution scheme was used to obtain good convergence and boundedness.

To eliminate the effect of grid size on numerical simulation results, a grid-independence analysis was performed on the impeller. Five models were computed under the same inlet pressure and temperature and the same outlet mass flowrate conditions, with only variation in the number of grid points. It can be observed in Fig. 6 that when the number of grid points reaches approximately 0.9 million, changes in efficiency can be considered negligible. The resultant total number of grid points of the impeller model was set at approximately 1 million.

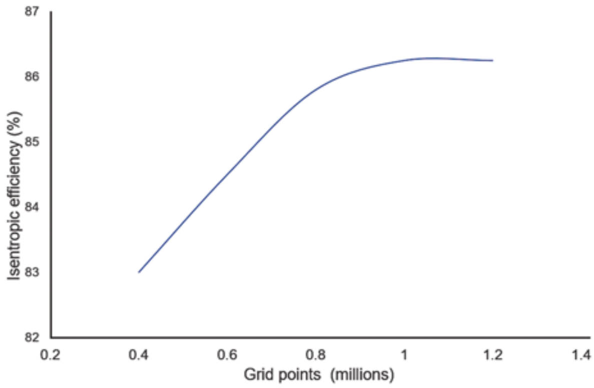

Fig. 6. Numerical results with different grid points

OVERALL PERFORMANCE

The overall performance of the radial impeller with vaneless diffuser of radius ratio of 1.18 at design speed is shown in Figs. 7 and 8. In these figures, the results computed in the present simulation are compared with the experimental and numerical results obtained by Prahst and Scotch. The pressure ratio predicted through Ansys CFX is quite close to the experiment and the value computed by Prahst and Scotch. The Ansys CFX computed efficiency is 86.4%, which is 0.3 points lower than the measured efficiency for the mass flow rate of 4.54 kg/sec, the same as the design value, and the total-to-total pressure ratio of 4.1. The computed performance curves are close to the experimental results, as shown in Figs. 7 and 8. The circumferentially averaged static pressure distribution computed by the author for the design flow rate is compared in Fig. 9 with the values experimentally measured and computed by Prahst and Scotch. The experimental measurements give the pressure distribution along the shroud, while the calculations give simple basic area-averages of the CFD results. The computed results are quite close to the measured static pressure distribution. However, in the vicinity of the impeller leading edge, the numerical simulation demonstrates higher impact of the leading edge than the experimental measurement.

The spanwise distributions of circumferentially averaged total pressure computed by the author for the radius ratio of 1.18 are compared in Fig. 10 with those experimentally measured and computed by Prahst and Scotch. Again, a good match is observed between the computed and measured data.

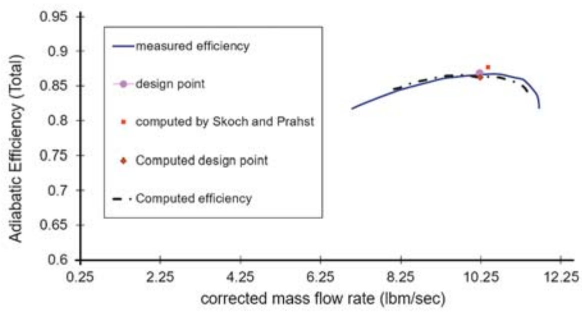

Fig. 7. Efficiency at radius ratio of 1.18

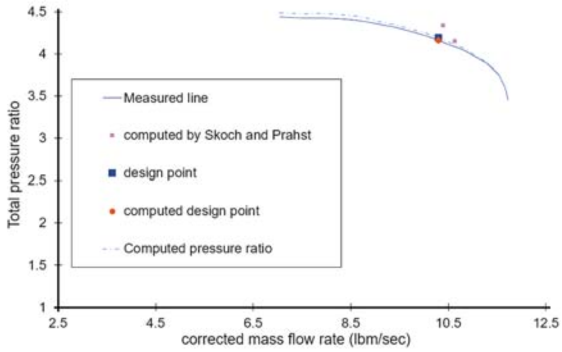

Fig. 8. Total pressure ratio at radius ratio of 1.18

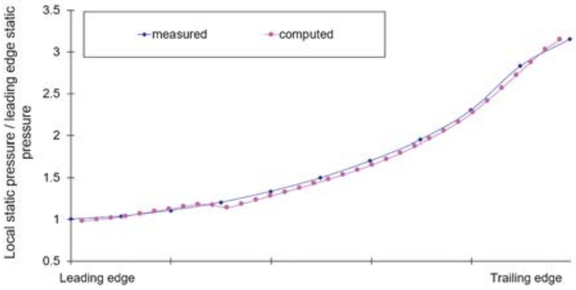

Fig. 9. Circumferentially averaged static pressure distributions

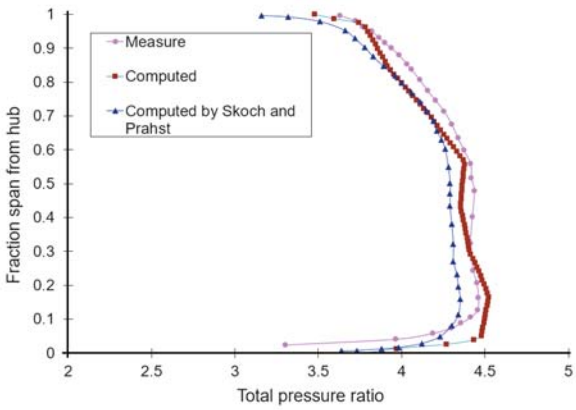

Fig. 10. Spanwise distributions of circumferentially averaged total pressure at radius ratio of 1.18

MODIFICATION OF MULTI SPLITTER BLADE

The abovementioned impeller was modified by adding a multi splitter to analyse its effect on the fluid flow in impeller passages and on overall performance of the impeller. The impeller was modified by keeping tip diameter, mass flow rate, rpm, theta and backswept definition, and thickness definition constant and the same as original. The impeller was modified with respect to big splitter and small splitter positions to observe their effect on the flow field. The original impeller had been designed with 15 full blades and 15 splitter blades. It was modified to 11 main blades, 11 small splitter blades, and 11 big splitter blades by keeping the theta, backswept, and thickness definitions as per original. In the modified design, the big splitter blades were situated close to the suction surfaces and the smaller splitter blades close to the pressure surfaces of the main blades. A number of splitter positions were analysed to obtain the maximum total pressure at constant flow rate and thus achieve higher efficiency. The splitter positions listed in Table 2 and 3 were selected after a number of hit and trial simulations aiming at efficiency and pressure ratio improvement.

Tab. 2. Positions of big and small splitter blades (spanwise from main blade suction surface)

	Big splitter	Small splitter
Modified impeller	0.4	0.7

Tab. 3. Positions of big and small splitter blades (normalized meridional length)

	m/m²	Modified impeller
Big splitter	hub	0.2
	shroud	0.22
Small splitter	hub	0.35
	shroud	0.37

The modified impeller was analysed with Ansys CFX, using the same computation procedure as for the original impeller. Figs. 11 and 12 show different views of the modified impeller.

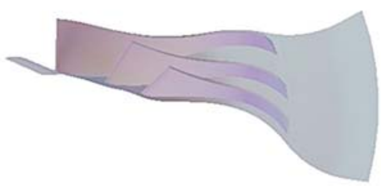

Fig. 11. 3D view of modified impeller

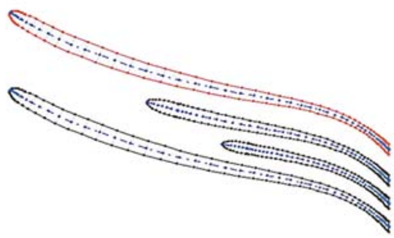

Fig. 12. Blade-to-blade view of modified impeller

EVALUATION OF MODIFIED IMPELLER

The performed CFD calculations have shown that increasing the number of main blades does not contribute to the increase in pressure ratio. What is worse, it deteriorates the impeller efficiency. A narrower blade passage, which increases the wetted area and accelerates the flow in the impeller, causes the increase in friction loss. That is why a decision was made to employ multi splitter blades which can reduce the Mach number at inducer with better efficiency. The aim was to compress the gas sequentially to higher pressure, thus bypassing the inlet Mach number limitation. It was observed that after adding the splitter, the total pressure ratio increased from 4.1 to 4.4, with simultaneous one percent efficiency increase. The streamwise distributions of circumferentially averaged total pressure computed for the original and modified impeller are shown in Fig. 13. At the leading edges, the original impeller has 15 blades while the modified impeller has 11 blades, therefore the pressure increase is higher in the original impeller. However, at the 20% streamwise distance, the action of the first splitter increases the pressure in the modified impeller, and then, further increase is generated by the second splitter at the 28% distance, all this leading to higher pressure ratio at the trailing edge. Resultantly, the modified impeller has higher pressure ratio, as the air is compressed sequentially. The pressure is raised by means of increase in pressure coefficient. However, the relative Mach number at the compressor leading edges is reduced after decreasing the number of main blades. The placement of splitters is more efficient than full blades, and the static pressure increase mainly happens when the flow past both the splitters and the main blades exists. The friction loss due to higher velocity gradient in the original impeller is reduced, as the velocity and the Mach number on blade surfaces are lower in the modified impeller. Once the circumferential width of the flow path passage is reduced due to the presence of splitter blades, the speed difference caused by the Coriolis force is also reduced, which increases the flow velocity in the radial direction.

The meridional velocity distributions in the original and modified impeller at 10% chord are shown in Fig. 14. It is observed that this velocity is reduced at inlet. It can be seen that with the addition of splitters, the flow separation decreases. The modification of splitter blades makes that the friction loss due to higher velocity gradient in the original impeller is reduced, as the velocity and the Mach number on blade surfaces are lower in the modified impeller, as shown in the 50% span entropy contour in Figs. 15 and 16. Additionally, the friction loss is reduced due to a smaller number of full blades. The tip leakage flow is also reduced, which leads to the reduction of flow separation near the trailing edges. The tip leakage loss is reduced due to a smaller number of main blades. In the original impeller, a higher relative Mach number is observed, as the splitter blade leading edges act towards limiting the flow between the splitter blade and the pressure side of the full blade. In the modified impeller, a smaller number of full blades makes that the separation phenomena do not exist and the fluid flows without any separation, as the effect of leading edge disturbance does not affect it. This indicates that the choking margin is increased in the modified impeller. The throat effect is also reduced remarkably. Actually, the high total pressure zone is larger when compared to the original impeller. All this results in higher efficiency.

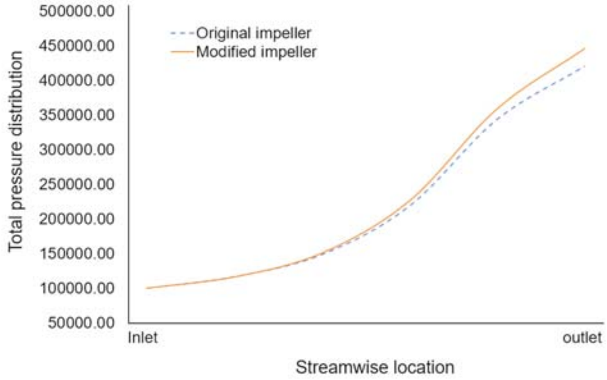

Fig. 13. Streamwise distributions of circumferentially averaged total pressure

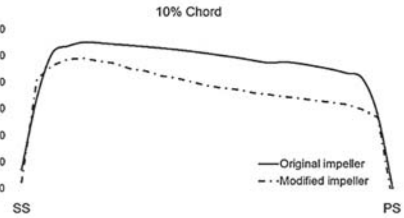

Fig. 14. Meridional velocity distributions at 10% chord and 50% span in cascade of original and modified impeller

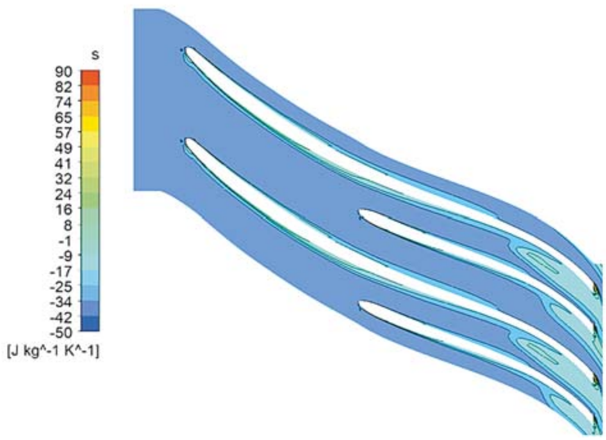

Fig. 15. Original blade contour of entropy at 50% span

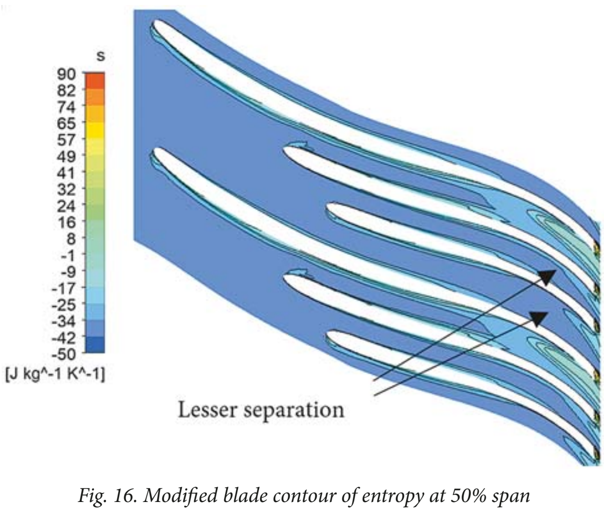

Fig. 16. Modified blade contour of entropy at 50% span

The contours of meridional velocity-to-tip speed ratio and relative Mach number at trailing edge for the original and modified impeller are shown in Figs. 17 to 20. A visibly smaller Mach number, along with more uniform flow and higher pressure, is observed in the big splitter and small splitter passages of the modified impeller. The jet and wake flows are visible in both impellers. It is shown that the wake core in each impeller is located near the splitter pressure side and close to the shroud side. However, in the modified impeller the jet flow in the passage between the small splitter and the big splitter differs slightly from that between the main blade and the big splitter in the original impeller. The wake zones are smaller near shroud and trailing edges due to less intensive separation in the presence of splitter blades and higher number of trailing edges.

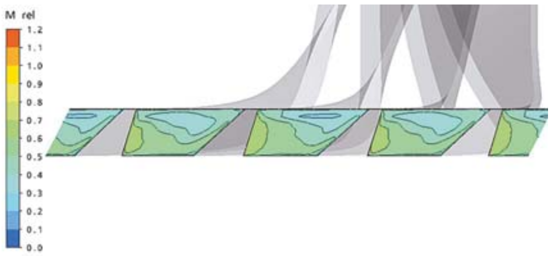

Fig. 17. Original blade contour of M rel at trailing edge

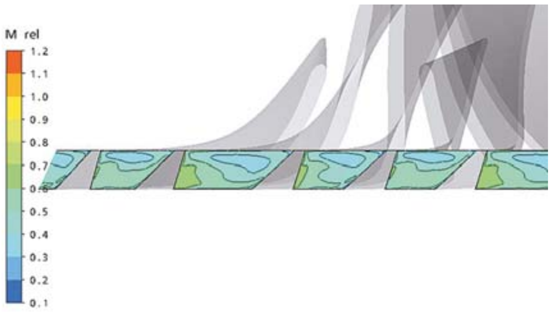

Fig. 18. Modified blade contour of M rel at trailing edge

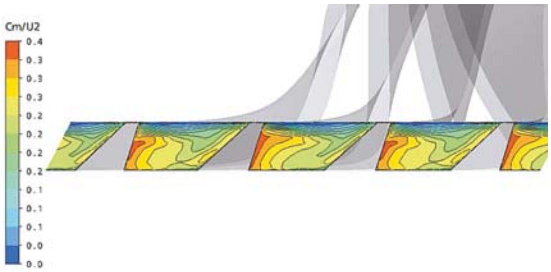

Fig. 19. Original blade contour of meridional velocity- to-tip speed ratio at trailing edge

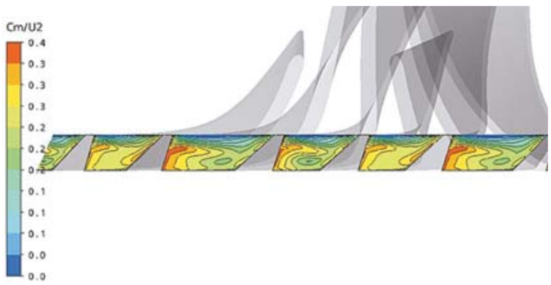

Fig. 20. Modified blade contour of meridional velocity- to-tip speed ratio at trailing edge

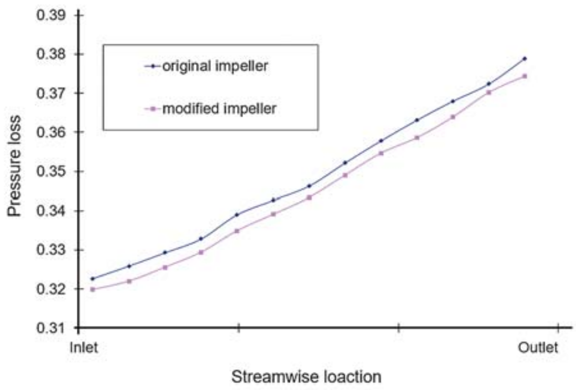

Fig. 21. Pressure losses in original and modified impeller

The pressure loss is defined as:

$$\text{Pressure loss} = \frac{P_t - P}{0.5\rho W_{inlet}^2}$$

where P_t is the mass average total pressure, ρ is the mass average density at inlet, and W is the mass average relative velocity at inlet.

The pressure losses in the original and modified impellers are shown in Figs. 21 to 25. Fig. 21 compares the average pressure losses in the original impeller and the modified impeller in the streamwise direction. It is observed that the pressure loss in the modified impeller is smaller than that in the original impeller. The same tendency can be observed in the pressure loss distributions on the main blade suction and pressure surfaces in the original and modified impeller, Figs. 22 to 25. The static pressure increase due to centrifugal acceleration is higher in the modified impeller. Thus, the static pressure retrieval capability in the modified impeller is increased. The impeller outlet static pressure retrieval is proportional to the effective portion of total diffusion ratio. It plays critical role in establishing high pressure recovery at smaller pressure loss. The pressure loss near the leading edge is smaller in the modified impeller. The figures show remarkable loss decrease near the pressure surface, and slight increase near the suction surface, which may be due to the effect of loss from the big splitter leading edge. Near the hub section, the low total pressure zone near the main blade is smaller in the modified impeller. For the midspan and near-tip sections, we can see that the low-pressure region is also smaller in the modified impeller.

A significant performance improvement is observed in the modified impeller. Not only the elevated entropy area is reduced, but also more uniform fluid flow is observed at impeller inlet and exit. The uniform flow benefits the downstream components of the compressor. The smaller low total pressure zone indicates that the impeller loss is lower and the impeller efficiency higher. The flow field distributions agree with the overall efficiency. The shroud low total pressure zone is smaller in the modified impeller, which indicates that this impeller has more uniform flow field and produces less mixing loss at downstream. Therefore, it has better impeller efficiency, which also benefits the overall efficiency. The flow

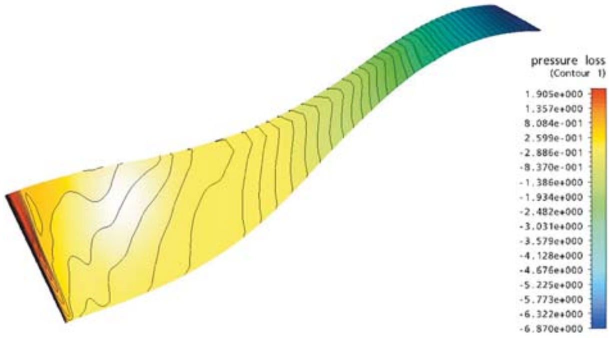

Fig. 22. Pressure loss on original impeller's main blade suction surface

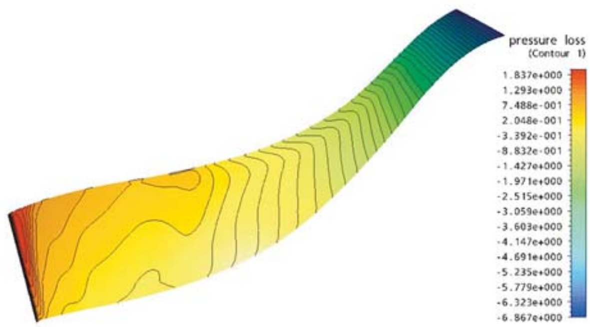

Fig. 23. Pressure loss on modified impeller's main blade suction surface

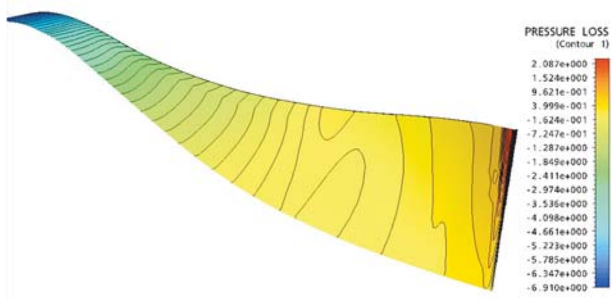

Fig. 24. Pressure loss on original impeller's main blade pressure surface

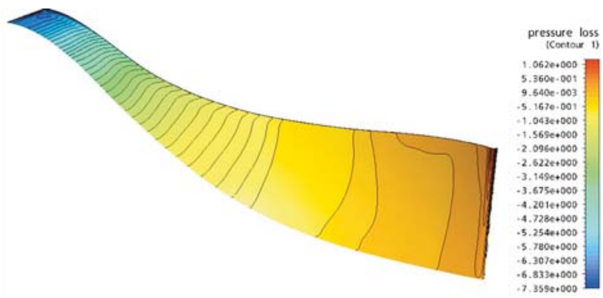

Fig. 25. Pressure loss on modified impeller's main blade pressure surface

is more uniform at the exit of the modified impeller, as it has less mixing loss, and benefits the aerodynamic performance of the downstream components. The placement of splitters is more efficient than full blades, and the static pressure increase mainly happens when the flow past both the splitters and the main blades exist. This also benefits the efficiency and the pressure ratio. The friction loss due to higher velocity gradient in the original impeller is reduced in the modified impeller, as the velocity and the Mach number on blade surfaces are lower. In addition, once the circumferential width of the flow path passage is reduced due to the presence of splitter blades, the speed difference caused by the Coriolis force is also reduced, which increases the flow velocity in the radial direction.

CONCLUSION

The reported study indicates that splitter positions have impact on the compressor stage performance, which is improved when the gas is compressed systematically with the alteration in location of splitters, from big to small splitters in cascade. The overall impeller performance is improved after adding a big splitter close to the suction surface and a small splitter close to the pressure surface of the main blade to reduce flow separation. It was observed that after installing the multi splitter, the total pressure ratio is increased from 4.1 to 4.4 with simultaneous one percent efficiency increase. Hence, the addition of a set of small and big splitter blades increases the pressure ratio and the efficiency of the centrifugal compressor impeller by reducing the pressure loss and generating a more uniform flow in the impeller cascade.

REFERENCES

1. C. Xu, R. S. Amano: *Numerical simulation of the aerodynamic effects on sweep compressor blades*, 2004, IGTI-2004-53008.

2. C. Xu and R. S. Amano: *A study of a single stage centrifugal compressor*, ASME Electric Power Conference 2006, PWR2006-88023, Georgia World Congress Centre, Atlanta, GA.

3. C. Xu and R. S. Amano: *Computational analysis of Scroll tongue shapes to compressor performance by using different turbulence models*, 2007, GT2007-28224.

4. C. Xu and R. S. Amano: *Development of a low flow coefficient single stage centrifugal compressor*, International Journal for Computational Methods in Engineering Science and Mechanics, 2009, 10(4), 282–289.

5. C. Xu, R. S. Amano: *Study of the flow in a centrifugal compressor*, Int. J. of Fluid Machinery and System, 2010, 3(3), 260–270.

6. C. Xu, R. S. Amano: *Meridional considerations of the centrifugal compressor development*, International Journal of Rotating Machinery, 2012, 1-11, doi:10.1155/2012/518381.

7. C. Xu, R. S. Amano: *Empirical design considerations for industrial centrifugal compressors*. International Journal of Rotating Machinery, 2012, 1-15, doi./10.1155/2012/184061.

8. Dean R.: *On the unresolved fluid dynamics of the centrifugal compressor*, Advanced Centrifugal Compressors, 1971, ASME Publications.

9. Fradin, C: *Investigation of the three-dimensional flow near the exit of two backswept transonic centrifugal impellers*, Proc. of the Eighth International Symposium in Air Breathing Engines, 1987, 149–155.

10. Hathaway M. J., Chriss R. M., Wood J. R., Strazisar A. J.: *Experimental and computational investigation of the NASA low-speed centrifugal compressor flow field*, ASME J. of Turbomachinery, 1993, Vol. 115, pp. 527–542.

11. Hirofumi Hattori, Tomoya Houra, Amane Kono and Shota Yoshikawa: *Computational fluid dynamics study for improvement of prediction of various thermally stratified turbulent boundary layers*, J. Energy Resour. Technol., 2017, 139 (5): 051209-051209-8.

12. Kano F., Tazawa N., Fukao Y.: A*erodynamic performance of large centrifugal compressors*, 1982, ASME Paper 82-GT-17.

13. Krain H.: *A study on centrifugal impeller and diffuser flow*, Transactions of the ASME, 1981, Vol. 103, pp. 688–697.

14. Masanao Kaneko, Hoshio Tsujita: *Influences of tip leakage flows discharged from main and splitter blades on flow field in transonic centrifugal compressor stage*, 2018, ASME Turbo Expo 2018, Vol. 2B, Paper GT 2018-75345.

15. M. Zangeneh: *On 3D design of centrifugal compressor impellers with splitter blades*, 1998, ASME paper 98-GT-507.

16. McKain T. F., Holbrook G. J.: *Coordinates for a high performance 4:1 pressure ratio centrifugal compressor*, NASA Contract NAS 3-23268, 1982, (to be published as a NASA CR).

17. Millour, V.: *3D Flow Computations in a Centrifugal Compressor with Splitter Blade Including Viscous Effect Simulation*, 16th Congress, International Council for Aeronautical Societies, 1988, 1, 842–847.

18. Moore J., Moore J. G., Timmis, P. H.: *Performance evaluation of centrifugal compressor impellers using three-dimensional viscous flow calculations*, J. of Engineering for Gas Turbines and Power, 1984, Vol. 106, pp. 475–481.

19. Ona, M., Kawamoto, H., Yamamoto, Y.: *Approach to high performance transonic centrifugal compressor*, 2002, AIAA 2002–3536.

20. Skoch G. J., Prahst P. S., Wernet M. P., Wood J. R., Strazisar A. J.: *Laser anemometer measurements of the flow field in a 4:1 pressure ratio centrifugal impeller*, 1997, ASME Paper 97-GT-342.

21. Tamaki, H., Yamaguchi, S., Nakao, H., Yamaguchi, H., Ishida, K., Mitsubori, K.: *Development of compressor for high-pressure ratio turbocharger*, 1998, IMechE C554/002.

22. Teipel I. and Wiedermann, A.: *Computation of flow fields in centrifugal compressor diffusers with splitter vanes*, Proc. of the International Gas Turbine Congress, 1987, 2, 311–317.

23. Vavra, M. H.: *Basic Elements of Advanced Design of Radial-Flow Compressors*, AGARD Lecture Series No. 89 on "Advanced Compressors, 1970".

CONTACT WITH THE AUTHORS

Adil Malik
e-mail: adilmalik99@hotmail.com

Harbin Engineering University
145 Nantong Street, 150001 Harbin
China

Qun Zheng
e-mail: zhengqun@hrbeu.edu.cn

Harbin Engineering University
145 Nantong Street, 150001 Harbin
China

Shafiq R. Qureshi
e-mail: shafique@pnec.nust.edu.pk

National University of Sciences and Technology
Habib Rehmatullah Road, 75300 Karachi
Pakistan

Salman A. Ahmed
e-mail: ahmedsalman18@yahoo.com

Harbin Engineering University
145 Nantong Street, 150001 Harbin
China

D. KB Gambo
e-mail: nagari2010@gmail.com

Harbin Engineering University
145 Nantong Street, 150001 Harbin
China